ADEOS-2 GLI Calibration Activities

JAXA GLI Calibration Group:

K. Tanaka[a], H. Murakami[a], S. Kurihara[a] , J. Inoue[a], Y. Okamura[a], K. Isono[a], J. Nieke[a], T. Hashimoto[a], H. Yamamoto[a], I. Asanuma[a], K. Iwafune[b], Y.Aoki[b], H. Yatagai[b], H. Kurihara[b], M. Yoshida[c], N. Sekio[c], Y. Mitomi[c], and Y. Senga[d], [a]*Japan Aerospace Exploration Agency (JAXA),* [b]*Fujitsu Ltd,* [c]*RESTEC,* [d]*Tokai Univ.*

Solar Calibration

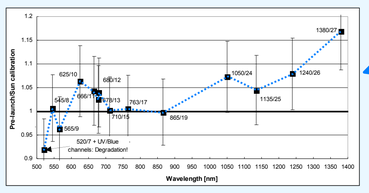

Pre-launch gain (K_{pre}/K_{sun}) derived using solar diffuser BRDF data (Nieke et al., SPIE, 2003)

Temporal change of K_{pre}/K_{sun} after correction of diffuser incident angle and sun-earth distance (scan-mirror side B, EL=15deg, normalized by 06 Apr. 2003).

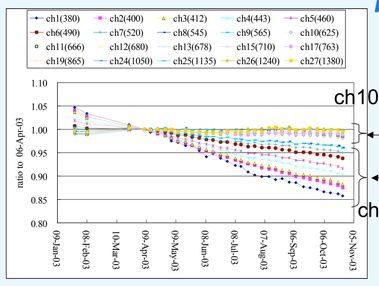

- Solar calibration outputs dropped in channels under 700nm. We consider this is caused by degradation of diffuser.
- Other channels are stable within 2%.
- The ratio of mirror side B to A increase after launch, and decreased gradually in orbit. It is considered that reflectance of side A decreased after launch by some reason, and recovered gradually.

Image Characterization and Correction

Correction of stripe-pattern noise

The de-striping coefficients $a_{k,l,j}$ are applied to Level-1B radiance after the all other radiometric calibrations, $L_{k,l,j}$.

$L_{k,l,j}^{corrected} = a_{k,l,j} L_{k,l,j}$, *(k: pixels, l: lines, j: bands)* **(1)**

We assume $a_{k,l,j}$ are related to input radiance $L_{k,l,j}$ and scan-mirror incident angle $\phi_{k,l}$.

$a_{k,l,j} = b0_{i,j} + b1_{i,j} \cdot L_{k,l,j} + b2_{i,j} / L_{k,l,j} + b3_{i,j} \cdot L_{k,l,j}^2 + b4_{i,j} \cdot \phi_{k,l} + b5_{i,j} \cdot \phi_{k,l}^2$, **(2)**

i: detectors (1-12 or 48 × scan-mirror sides), i=mod(l-1, 24 or 96)+1.

Non-linearlity, over saturation and tailing

- Non-linearity table for ch14, 16, 18 is updated using solar calibration data.
- Over saturation and tailing are flagged using neighboring low-gain channels.

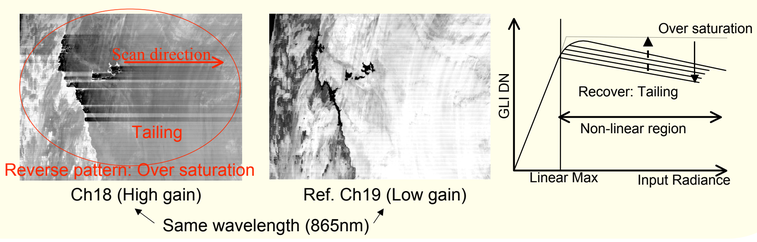

JAXA GLI calibration sub-groups

Group 1 ***Solar & internal lamp calibrations***

Group 2 ***Blackbody calibration***

Group 3 ***Geometric correction***

Group 4 ***General L1 characterization***

Group 5 ***Vicarious calibration & Cross calibration***

Group 6 ***Level-1 software development***

Lamp Calibration

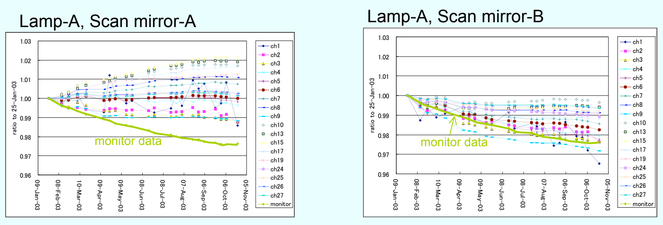

Lamp calibration raw data from 1st lamp calibration in Jan. 2003.

- Raw data of mirror side A increased, and ones of mirror side B decreased.
- Data corrected by monitor diode is increased in both mirror sides, so decrease of raw data level in mirror side B is considered to be caused by lowering of lamp radiance.
- Corrected data of mirror side-B increased only 1%.
- The ratio of side B to A increased after launch, so the reflectance of side A is thought to be decreased (about 4%) due to the influence of launch, but recovered since then.
- Noise level of the lamp data is equivalent to the pre-launch test.

Vicarious Calibration

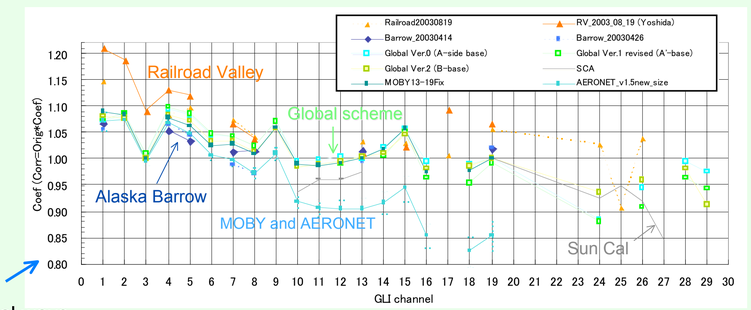

GLI vicarious calibration coefficients (*Kvc*) by several ways

- Using global datasets, we derived dependencies on scan-mirror A/B sides, incident angle (φ), and observation date (T).

Kvc at CHs 1-3 for each φ and T by the global scheme. Colors indicate T from 6 Feb. to 24 Oct.; circles, average Kvc for each 5-deg φ bin.

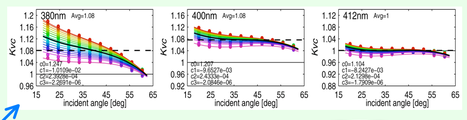

Cooperation with GLI Validation Group

Blackbody Calibration

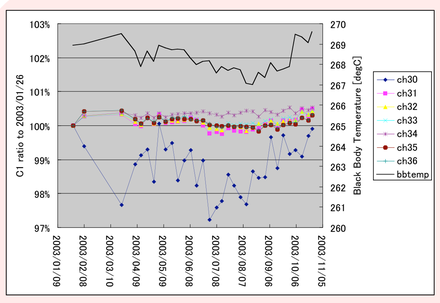

Linear part of the black body calibration (C1) at the same sun elevation point (20deg).

GLI thermal data is calibrated by the C1 (for each scan) and fixed calibration factors (C0, C2, and other environmental factors) derived in the pre-launch tests.

- C1 was stable over all operation period within ±3% at ch30, and other channels within ±1%.
- C1 changed corresponding Blackbody temperature, so it is considered that the change is caused by the seasonal variation of environmental temperature.
- C1 was smaller (= higher sensitivity) in cold environment in orbit. This agrees the pre-launch test results.
- Calculated NEΔT and dynamic range is within specification.

Geometric calibration

- Band-to-band registration of L1A
- GCP extraction from L1A images
- Correction of Sat/GLI Alignment
- Correction of detector address
- Correction of mirror-side A/B alignments
- Geometric accuracy by system correction (without GCPs): about 1.5 pixels (250m) [about 1 pixel (1km)]
- Precise geometric correction (with GCPs, for land product): less than 1 pixel (250m, 1km)

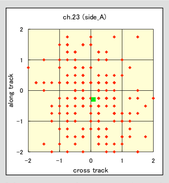

Along and cross track deviations from GCP (250m CH23).

Cooperation with GLI Land group

Version up & processing information

Earth Observation Center (EOC)
Data distribution to public

http://www.eoc.jaxa.jp/homepage.html

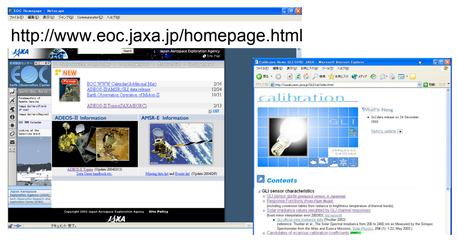

Earth Observation Research and Application Center (EORC)
Research &Level-2 information and sample data

http://suzaku.eorc.jaxa.jp/GLI/cal/index.html

Global Imager (GLI) system overview

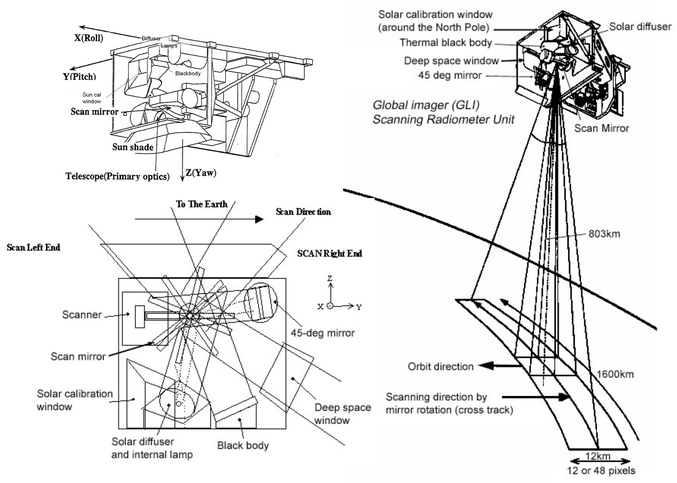

Table 1 Characteristics of GLI channels

Ch	*WL*[*4] *[nm]*	*Width*[*4] *[nm]*	*Dynamic range [W/m²/str/μm]*	*SNR*[*5] *(input level)*	*IFOV [m]*	*Ch*	*WL*[*4] *[nm]*	*Width*[*4] *[nm]*	*Dynamic range [W/m²/str/μm]*	*SNR*[*5] *(input level)*	*IFOV [m]*
1	380.7	10	683	467 (59)	1000	20	462.4	62	691	241 (36)	250
2	399.6	9	162	1286 (70)	1000	21	542.1	48	585	141 (25)	250
3	412.3	10	130	1402 (65)	1000	22	661.3	59	107	255 (14)	250
4	442.5	9	110[*1] /680	893 (54)	1000	23	824.1	103	235 (210[*3])	218 (21)	250
5	459.3	9	124[*1] /769	880 (54)	1000	24	1048.6	20	227	381 (8)	1000
6	489.5	11	64	1212 (43)	1000	25	1136.6	69	184	412 (8)	1000
7	519.2	10	92[*1] /569	627 (31)	1000	26	1241.0	18	208	303 (5.4)	1000
8	544.0	10	96[*1] /596	611 (28)	1000	27	1380.6	36	153	192 (1.5)	1000
9	564.8	10	39	1301 (23)	1000	28	1644.9	203	76	298 (5)	250[*2]
10	624.7	10	32 (28[*3])	1370 (17)	1000	29	2193.8	220	32	160 (1.3)	250[*2]
11	666.7	10	21	1342 (13)	1000	*Ch*	*WL*[*4] *[nm]*	*width [nm]*	*Dynamic range [Kelvin]*	*NEΔT [K] at 300K*	*IFOV [m]*
12	679.9	10	22	1293 (12)	1000						
13	678.6	10	342[*3]	235 (12)	1000	30	3721.1	336	345	0.07	1000
14	710.5	11	16	1404 (10)	1000	31	6737.5	531	307	0.03 (at 285K)	1000
15	710.1	11	233[*3]	300 (10)	1000	32	7332.6	502	322	0.03	1000
16	749.0	11	11	991 (7)	1000	33	7511.4	526	324	0.02	1000
17	762.0	8	246[*3]	293 (6)	1000	34	8626.3	519	350	0.05	1000
18	866.1	20	8	1309 (5)	1000	35	10768.0	955	354	0.05	1000
19	865.7	10	211[*3]	386 (5)	1000	36	12001.3	1020	358	0.06	1000

*1 Knee points of the piece-wise linear gain channels 4, 5, 7, and 8.
*2 Channels 28 and 29 are re-sampled for each 2-km (1/8) on board and stored in the 1-km level-1B product.
*3 Maximum radiance for linear response.
*4 Channel center and width are derived from GLI spectral response.
*5 SNR at the standard input level (W/m2/sr/μm) was measured in pre-launch evaluation tests.